Int J Fract (2006) 141:63–73
DOI 10.1007/s10704-006-0062-y

ORIGINAL ARTICLE

On the dynamic behaviour of interfacial cracks between a piezoelectric layer and an elastic substrate

G. L. Huang · X. D. Wang

Received: 4 June 2005 / Accepted: 13 March 2006

Abstract Surface-bonded piezoelectric layers can be used as actuators/sensors for advanced structural applications. The current paper provides a theoretical study of the dynamic behaviour of interacting cracks between a piezoelectric layer and an elastic medium under antiplane mechanical loads. The electromechanical field of a single interfacial crack is determined first using Fourier transform technique and solving the resulting integral equations. This fundamental solution is then implemented into a pseudo-incident wave method to account for the interaction between different cracks. The dynamic behaviour of the resulting stress field is studied with special attention being paid to the stress intensity factors at the crack tips. Typical examples are provided to show the effect of the size and position of the cracks, the material combination and the loading frequency upon the stress intensity factors.

Keywords Interface · Crack · Piezoelectric layer · Dynamic behaviour · Interaction

G. L. Huang · X. D. Wang (✉)
Department of Mechanical Engineering,
University of Alberta, Edmonton, Alberta,
Canada T6G 2G8
e-mail: xiaodong.wang@ualberta.ca

1 Introduction

Due to their advantages of quick response, low power consumption, high linearity and strong electromechanical coupling, piezoelectric materials have been extensively used as actuators and sensors to form smart systems in the design of advanced structures (Gandhi and Thompson 1992; Chee et al. 1998; Bar-Cohen 2000; Boller 2000). In these applications, piezoelectric actuators/sensors are usually surface-mounted and the actuation/sensing process is controlled by the load transfer through the interfaces. Any interfacial debonding between these actuators/sensors and the host structure may significantly degrade their efficiency. The determination of the electromechanical behaviour of interfacial debonding in integrated smart structures is, therefore, an important issue in the design of this type of structures.

The quasi-static electromechanical behaviour of cracks in piezoelectric materials has been extensively studied. There are two typical crack models using different electric boundary conditions along the crack surfaces, which have been extensively used to study the fracture behaviour of piezoelectric materials. One is the electrically permeable crack model (Parton 1976; Beom 2003), and the other is the electrically impermeable model (Deeg 1980; Pak 1990, 1992; Suo et al. 1992; Park and Sun 1994). For the permeable crack model, both electric displacement and electric potential are

continuous across the crack surfaces. For the impermeable crack model, a charge-free condition along the crack faces is assumed. Based on these models, the behaviour of interacting cracks in piezoelectric media (Pak and Goloubeva 1995; Chen and Han 1999a, b; Han and Wang 1999) and interfacial cracks between a piezoelectric actuator and an elastic substrate have been analysed (Liu and Hsia 2003).

New piezoelectric materials have shown great potential as actuators/sensors in high-frequency applications. Correspondingly, the dynamic behaviour of cracks in piezoelectric materials have received significant attention from the research community. Shindo and Ozawa (1990) investigated the steady state dynamic response of cracked piezoelectric materials subjected to incident plane harmonic waves. Chen and Karihaloo (1999) studied the transient response of a finite crack in an infinite piezoelectric medium under the antiplane mechanical loads and inplane electric displacements using the integral transform method. Norita and Shindo (1999) investigated the scattering of antiplane shear waves by a finite crack in piezoelectric laminates. Li and Mataga (1996a, b) studied the problem of a semi-infinite, antiplane crack propagating in an infinite piezoelectric medium to evaluate the effect of the speed of the crack propagation on the crack tip fields. Li et al. (2000) considered a moving mode-III impermeable crack at the interface between two dissimilar piezoelectric half-spaces. Wang et al. (2000) analysed the transient response of a crack perpendicular to the edges of a piezoelectric strip subjected to dynamic antiplane mechanical and electrical loads. Meguid and Wang (1998) and Wang and Meguid (2000) studied the dynamic interaction of arbitrarily oriented cracks in piezoelectric media under different electric boundary conditions subject to incident antiplane shear waves. Wang (2001) investigated the dynamic behaviour of interacting interfacial cracks between two semi-infinite piezoelectric media subject to antiplane mechanical loads. Zhao and Meguid (2002) studied the dynamic behaviour of a piezoelectric laminate containing multiple interfacial collinear cracks subjected to steady state electromechanical loads based on both permeable and impermeable crack models.

A piezoelectric element used in smart structural applications may undergo different deformations depending on the design of the system. Two typical possible deformation modes are thickness expansion and thickness shear when the polarization direction of the piezoelectric element is parallel to and perpendicular to the thickness direction, respectively, corresponding to inplane and antiplane deformation.

Of particular interest in the current work is the antiplane dynamic debonding of piezoelectric thin sheets from elastic host media. The objective is to provide a theoretical study of interacting interfacial cracks between a thin piezoelectric layer and an elastic substrate subjected to incident Love waves, which propagate along the layer. The theoretical formulations governing the problem are based upon the use of the integral transform technique and a pseudo-incident wave method. The resulting dynamic stress intensity factors at the interacting cracks are obtained by solving the resulting singular integral equations using Chebyshev polynomial expansions at different loading frequencies. Numerical simulation is conducted to study the effects of the sizes and locations of the cracks, the material properties and the loading frequency upon the fracture behaviour of interacting cracks.

2 Formulation of the problem

Consider the problem of a piezoelectric layer bonded to a homogeneous isotropic elastic medium with multiple interfacial cracks. The piezoelectric layer is assumed to be very thin in comparison with the thickness of the host medium and, therefore, the host medium is assumed to be semi-infinite. The system is subjected to a harmonic antiplane incident wave of frequency ω, as shown in Fig. 1. A global Cartesian coordinate (x, y, z) and M local systems $(x_n, y_n, z_n), n = 1, 2, \ldots, M$ are employed to characterize different cracks. The position of the centre of crack n is given by $x = X_n,\ y = 0$ in the global coordinate system. The piezoelectric layer, with the z-axis being the polarization direction, occupies a region $-h < y < 0, -\infty < x < \infty$ with h being the thickness of the piezoelectric layer. The steady state mechanical fields corresponding to the

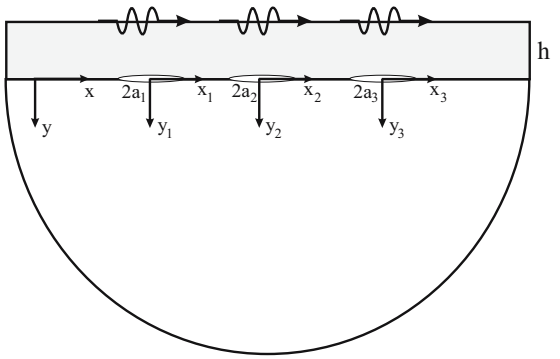

Fig. 1 Interacting cracks between a piezoelectric layer and an elastic medium

incident wave will generally involve an exponential harmonic factor $e^{-i\omega t}$. For the sake of convenience, the exponential harmonic factor will be suppressed and only the amplitude of different field variables will be considered.

The dynamic electromechanical behaviour of a homogeneous piezoelectric material under harmonic antiplane mechanical loading is fully described, as shown in Appendix, by the following governing equations,

$$c_{44}\nabla^2 w + e_{15}\nabla^2\phi + \rho\omega^2 w = 0, \tag{1}$$

$$e_{15}\nabla^2 w - \kappa_{11}\nabla^2\phi = 0, \tag{2}$$

where the Laplacian operation ∇^2 stands for $\partial^2/\partial x^2 + \partial^2/\partial y^2$, w is antiplane displacement and ϕ is the electric potential. ρ is the mass density of the piezoelectric material, c_{44}, e_{15} and κ_{11} are the elastic modulus, the piezoelectric constant and the dielectric constant of the piezoelectric layer, respectively. Introducing a new function given by

$$f = \frac{e_{15}}{\kappa_{11}}w - \phi, \tag{3}$$

Eqs. 1 and 2 can be reduced to

$$\nabla^2 w + k^2 w = 0, \quad \nabla^2 f = 0, \tag{4}$$

where k is the wave number defined by

$$k^2 = \frac{\rho\omega^2}{c^*}, \qquad c^* = c_{44} + \frac{e_{15}^2}{\kappa_{11}}. \tag{5}$$

The corresponding non-vanishing stress and electric displacement components are given as

$$\tau_{yz} = c^*\frac{\partial w}{\partial y} + e_{15}\frac{\partial f}{\partial y}, \quad \tau_{xz} = c^*\frac{\partial w}{\partial x} + e_{15}\frac{\partial f}{\partial x}, \tag{6}$$

$$D_x = -\kappa_{11}\frac{\partial f}{\partial x}, \quad D_y = -\kappa_{11}\frac{\partial f}{\partial y}, \tag{7}$$

where τ_{xz} and τ_{yz} are the shear stress components, D_x and D_y are the electric displacements.

The constitutive relation for the elastic host medium can be written as

$$\tau_{xz}^1 = c_{44}^1\frac{\partial w^1}{\partial x}, \qquad \tau_{yz}^1 = c_{44}^1\frac{\partial w^1}{\partial y}, \tag{8}$$

where τ_{xz}^1 and τ_{yz}^1 are the shear stress components, w^1 and c_{44}^1 are the displacement and the shear modulus of the host medium, respectively, with the superscript '1' indicating the host medium. The governing equation is given by

$$\nabla^2 w^1 + (k^1)^2 w^1 = 0 \tag{9}$$

in which $k^1 = \dfrac{\omega}{c^1}$ with $c^1 = \sqrt{c_{44}^1/\rho^1}$ and ρ^1 is the mass density of the host medium.

3 Solution of single interfacial crack problem

Consider now the steady state antiplane shear problem of a single crack of length $2a$ between a piezoelectric layer and a host medium subjected to harmonic mechanical loads. In the framework of linear theory, the problem can be decomposed into two subproblems, (1) a crack-free system subjected to the incident wave, and (2) the cracked system subjected to boundary loads along the crack surfaces. The wave propagation in the crack-free structure has been investigated by Wang et al. (2001). The resulting stress τ^I at the site of the crack will be used as the boundary load along the crack surfaces in subproblem (2) to ensure the traction free condition of the original problem at the crack. Therefore, subproblem (2) should satisfy the following mechanical boundary conditions:

$$\tau_{yz}(x,-h) = 0,$$

$$\tau_{yz}^1(x,0) = \tau_{yz}(x,0), \quad -\infty < x < \infty, \tag{10}$$

$$\tau_{yz}(x,0) = -\tau_{yz}^I(x,0), \quad -a < x < a, \tag{11}$$

$$w(x,0) = w^1(x,0), \quad |x| > a. \tag{12}$$

The electric boundary condition of cracks in piezoelectric media has been the topic of many investigations (Dunn 1994; Zhang et al. 1998). For the current antiplane problem, since no opening displacement exists, the crack surfaces is assumed to

be in perfect contact. Accordingly, the permeable crack model is used, i.e. both the electric potential and the normal electric displacement are assumed to be continuous across the crack surfaces. It is further assumed that the host elastic material is a grounded conductor. The electric boundary condition of the crack problem can then be expressed as

$$\phi(x,0)=0, \quad -\infty<x<\infty. \tag{13}$$

By solving Eqs. 4 and 9 using Fourier transform with respect to x, the resulting wave field in the piezoelectric material and the host medium can be obtained as

$$w(x,y)=\int_{-\infty}^{\infty}[A_1(s)\mathrm{e}^{-\alpha y}+B_1(s)\mathrm{e}^{\alpha y}]\mathrm{e}^{-isx}\mathrm{d}s, \tag{14}$$

$$f(x,y)=\int_{-\infty}^{\infty}[A_2(s)\mathrm{e}^{-|s|y}+B_2(s)\mathrm{e}^{|s|y}]\times\mathrm{e}^{-isx}\mathrm{d}s, \tag{15}$$

$$w^1(x,y)=\int_{-\infty}^{\infty}A_3(s)\mathrm{e}^{-\alpha^1 y}\mathrm{e}^{-isx}\mathrm{d}s, \tag{16}$$

where $A_1(s)$, $A_2(s)$, $A_3(s)$, $B_1(s)$ and $B_2(s)$ are unknown functions of s and α and α^1 are given by

$$\alpha=\begin{cases}\sqrt{s^2-k^2}, & |s|>k\\ -i\sqrt{k^2-s^2}, & |s|<k\end{cases},$$

$$\alpha^1=\begin{cases}\sqrt{s^2-(k^1)^2}, & |s|>k^1,\\ -i\sqrt{(k^1)^2-s^2}, & |s|<k^1,\end{cases} \tag{17}$$

By using the boundary conditions (10) and (13), and defining the following dislocation density function

$$\psi(x)=\frac{\partial[w(x,0^+)-w^1(x,0^-)]}{\partial x}, \quad |x|\le a, \tag{18}$$

$A_1(s)$, $A_2(s)$, $A_3(s)$, $B_1(s)$ and $B_2(s)$ can be expressed in terms of one unknown function $\psi(s)$ as

$$A_1(s)=\Delta_1\psi(s), \qquad A_2(s)=\Delta_2\Delta_1\psi(s), \tag{19}$$

$$A_3(s)=\left[\Delta_1(1+\mathrm{e}^{2\alpha h})-\frac{i}{s}\right]\psi(s), \tag{20}$$

$$B_1(s)=\mathrm{e}^{2\alpha h}\Delta_1\psi(s),$$

$$B_2(s)=\mathrm{e}^{2|s|h}\Delta_2\Delta_1\psi(s), \tag{21}$$

where Δ_1 and Δ_2 are given by

$$\Delta_1(s)=\frac{ic_{44}^1\alpha^1}{sN}, \qquad \Delta_2(s)=-\frac{e_{15}(1+\mathrm{e}^{2\alpha h})}{\kappa_{11}(1+\mathrm{e}^{2|s|h})}, \tag{22}$$

$$N=(c^*\alpha+c_{44}^1\alpha^1)\mathrm{e}^{2\alpha h}-c^*\alpha+c_{44}^1\alpha^1 -\frac{e_{15}^2|s|}{\kappa_{11}}\frac{(1+\mathrm{e}^{2\alpha h})(\mathrm{e}^{2|s|h}-1)}{1+\mathrm{e}^{2|s|h}}. \tag{23}$$

The stress distribution along the interface can then be obtained as

$$\tau_{yz}(x,0)=\frac{c_{44}^1}{2\pi}\int_{-a}^{a}\psi(u)\int_{-\infty}^{\infty}i\alpha^1 \times\left[i\Delta_1(1+\mathrm{e}^{2\alpha h})+\frac{1}{s}\right]\mathrm{e}^{is(u-x)}\mathrm{d}s\,\mathrm{d}u. \tag{24}$$

The kernel of the infinite integration in Eq. 24 tends to a constant when $|s|\to\infty$, which corresponds to the singular term of the stress. After performing the appropriate asymptotic analysis, the following result can be obtained:

$$\beta_0=-\lim_{s\to\infty}\alpha^1\left[i\Delta_1(1+\mathrm{e}^{2\alpha_0 h})+\frac{1}{s}\right] =\frac{c_{44}}{c_{44}+c_{44}^1}. \tag{25}$$

By using the boundary condition given by Eqs. 11 and 12 and the asymptotic behaviour given by Eq. 25, a system of governing equations for determining ψ are obtained,

$$-\int_{-a}^{a}\psi(u)\int_{0}^{\infty}\left\{\frac{\alpha^1}{\beta_0}\left[i\Delta_1(1+\mathrm{e}^{2\alpha h})+\frac{1}{s}\right]+1\right\} \times\sin s(u-x)\mathrm{d}s\,\mathrm{d}u +\int_{-a}^{a}\frac{\psi(u)}{u-x}\mathrm{d}u=-\frac{\pi}{c_{44}^1\beta_0}\tau_{yz}^I(x), \quad |x|<a \tag{26}$$

and

$$\int_{-a}^{a}\psi(u)\mathrm{d}u=0. \tag{27}$$

Equation (26) is a singular integral equation of the first kind. Its solution includes the well-known square-root singularity and can be expressed as

$$\psi(u)=\sum_{j=0}^{\infty}c_jT_j(x/a)/\sqrt{1-x^2/a^2}, \tag{28}$$

where T_j are the Chebyshev polynomials of the first kind and c_j are unknown constants. From the orthogonality condition of the Chebyshev polynomials, Eq. 27 leads to $c_0=0$. Substituting Eq. 28 into Eq. 26, the following algebraic equation for c_j is obtained:

$$\sum_{j=1}^{\infty}c_jU_j(x/a)-\sum_{j=1}^{\infty}c_jg_j(x)=-\frac{1}{c_{44}^1\beta_0}\tau_{yz}^I(x), \quad |x|<a, \tag{29}$$

where U_j represent the Chebyshev polynomials of the second kind and

$$g_j(x) = \begin{cases} (-1)^n a \int_0^\infty \left\{ \frac{\alpha^1}{\beta_0} \left[i\Delta_1(1+\mathrm{e}^{2\alpha h}) + \frac{1}{s} \right] \right. \\ \quad \left. +1 \right\} J_j(sa)\cos(sx)\mathrm{d}s, \quad j = 2n+1, \\ (-1)^{n+1} a \int_0^\infty \left\{ \frac{\alpha^1}{\beta_0} \left[i\Delta_1(1+\mathrm{e}^{2\alpha h}) + \frac{1}{s} \right] \right. \\ \quad \left. +1 \right\} J_j(sa)\sin(sx)\mathrm{d}s, \quad j = 2n \end{cases} \tag{30}$$

in which J_j are the Bessel functions of the first kind. Truncating the Chebyshev polynomials in Eq. 28 to the Nth term and assuming that Eq. 29 is satisfied at N collocation points along the crack surface,

$$x_l = a\cos\left[\frac{l}{N+1}\pi\right], \quad l = 1,2,\ldots,N. \tag{31}$$

Equation (29) can be reduced to a system of linear algebraic equations of the following form

$$\sum_{j=1}^{\infty} c_j \frac{\sin\left(\frac{jl\pi}{N+1}\right)}{\sin\left(\frac{j\pi}{N+1}\right)} - \sum_{j=1}^{\infty} c_j g_j(x_l) = -\frac{1}{c_{44}^1\beta_0}\tau_{yz}^I(x_l), \quad j,l = 1,2,\ldots,N. \tag{32}$$

c_j can then be determined by solving the following equation,

$$[A]\{c\} = -\frac{1}{c_{44}^1\beta_0}\{\tau\}, \tag{33}$$

where

$$\{c\} = \{c_1,\ldots,c_j,\ldots,c_N\}^T, \tag{34}$$

$$\{\tau\} = \{\tau_{yz}^I(x_1),\tau_{yz}^I(x_2),\ldots,\tau_{yz}^I(x_j),\ldots,\tau_{yz}^I(x_N)\}^T \tag{35}$$

and

$$[A] = \begin{bmatrix} A_{11} & A_{12} & \cdots & A_{1N} \\ A_{21} & A_{22} & \cdots & A_{2N} \\ \vdots & \vdots & \vdots & \vdots \\ A_{N1} & A_{N2} & \cdots & A_{NN} \end{bmatrix} \tag{36}$$

with

$$A_{lj} = \frac{\sin\left(\frac{jl\pi}{N+1}\right)}{\sin\left(\frac{j\pi}{N+1}\right)} - g_j(x_l), \quad j,l = 1,2,\ldots,N. \tag{37}$$

Based on the solution given by Eq. 33, the stress distribution along the interface resulting from the crack can be obtained by substituting Eq. 28 into Eq. 24, such that

$$\tau_{yz}(x,0) = [h(a,x)]\{c\} \tag{38}$$

in which $[h(a,x)] = [h_1(a,x), h_2(a,x), \ldots, h_N(a,x)]$ and $h_j(a,x)$ are given by

$$h_j(a,x) = \begin{cases} (-1)^n a\beta_0 \int_0^\infty J_j(sa)\cos(sx)\mathrm{d}s, & j = 2n+1, \\ (-1)^{n+1} a\beta_0 \int_0^\infty J_j(sa)\sin(sx)\mathrm{d}s, & j = 2n, \end{cases}$$

$$- \begin{cases} (-1)^n a \int_0^\infty \left\{ \alpha^1 \left[i\Delta_1(1+\mathrm{e}^{2\alpha h}) + \frac{1}{s} \right] + \beta_0 \right\} \\ \quad J_j(sa)\cos(sx)\mathrm{d}s, \quad j = 2n+1, \\ (-1)^{n+1} a \int_0^\infty \left\{ \alpha^1 \left[i\Delta_1(1+\mathrm{e}^{2\alpha h}) + \frac{1}{s} \right] + \beta_0 \right\} \\ \quad J_j(sa)\sin(sx)\mathrm{d}s, \quad j = 2n \end{cases} \tag{39}$$

with

$$\int_0^\infty J_j(sa)\cos(sx)\mathrm{d}s = \frac{(-1)^{n+1}a^j}{\sqrt{x^2-a^2}[\sqrt{x^2-a^2}+|x|]^j}, \quad j = 2n+1, \tag{40}$$

$$\int_0^\infty J_j(sa)\sin(sx)\mathrm{d}s = \mathrm{sgn}(x)\frac{(-1)^{n+1}a^j}{\sqrt{x^2-a^2}[\sqrt{x^2-a^2}+|x|]^j}, \quad j = 2n. \tag{41}$$

4 Interaction between cracks

For the general cases where multiple interface cracks are involved, as shown in Fig. 1, the interaction between these cracks may significantly affect the local stress field around the crack tips. This interaction effect will be considered in this section using a pseudo-incident wave method based on the single interfacial crack solution. The technique developed by Wang and Meguid (1997) will be briefly described in the next section.

4.1 Pseudo-incident wave

For crack n, in addition to the initial stress τ_{yz}^I induced by subproblem (1), the crack will also

experience a stress τ_n^p caused by a scattered wave from other cracks, which can be regarded as an unknown incident wave, pseudo-incident wave. The behaviour of crack n can be equivalently described by a single interfacial crack subjected to an incident wave given by

$$\tau_n^I = \tau_{yz}^I + \tau_n^p. \tag{42}$$

In response to this incident wave, crack n will result in a scattered wave τ_n^{sc}. The total stress field can then be expressed as

$$\tau^{\mathrm{total}} = \tau_{yz}^I + \tau_n^p + \tau_n^{\mathrm{sc}}. \tag{43}$$

The total stress field can also be expressed by summing up the stress from the initial field and the contributions from all the cracks, such that

$$\tau^{\mathrm{total}} = \tau_{yz}^I + \sum_{m=1}^{M} \tau_m^{\mathrm{sc}}. \tag{44}$$

The equivalence between Eqs. 43 and 44 indicates that

$$\tau_n^p = \sum_{m\neq n}^{M} \tau_m^{\mathrm{sc}}, \quad n = 1,2,\ldots,M. \tag{45}$$

4.2 Solution of interacting cracks

Based on the single interfacial crack solution discussed in Sect. 3, the interfacial stress at point x due to crack m can be expressed, by using Eq. 38, as

$$\tau_m^{\mathrm{sc}}(x) = [h(a_m, x - X_m)]\{c\}^m, \tag{46}$$

where $\{c\}^m$ represents the coefficients of the Chebyshev polynomial expansion of crack m.

For any crack n, the interfacial stress acting on its surfaces induced by the pseudo-incident wave can be obtained by substituting Eq. 46 into 45 as

$$\tau_n^p(x_n) = \sum_{m\neq n}^{M} [h(a_m, x_n - X_m + X_n)]\{c\}^m. \tag{47}$$

We are interested in the shear stress at the following collocation points

$$x_n^l = a_n \cos\left[\frac{l}{N+1}\pi\right], \quad l = 1,2,\ldots,N. \tag{48}$$

By using Eqs. 47 and 48, the stress at these points due to the total incident wave of crack n can be obtained as

$$\{t\}_n = \{t\}_n^I + [Q]^n\{C\}, \tag{49}$$

where

$$\{t\}_n^I = \begin{Bmatrix} \tau_{yz}^I(x_n^1) \\ \tau_{yz}^I(x_n^2) \\ \vdots \\ \tau_{yz}^I(x_n^N) \end{Bmatrix}, \quad \{C\} = \begin{Bmatrix} \{c\}^1 \\ \{c\}^2 \\ \vdots \\ \{c\}^M \end{Bmatrix} \tag{50}$$

with $\{t\}_n^I$ being the initial stress due to subproblem (1) and $\{C\}$ being the coefficients of the Chebyshev polynomial expansion of interacting cracks. $[Q]^n$ represents the interaction between cracks and is given by

$$[Q]^n = \begin{bmatrix} 0 & & \\ f(a_1, x_n^2 - X_1 + X_n) & & \\ \vdots & & \\ f(a_1, x_n^N - X_1 + X_n) & & \end{bmatrix} \tag{51}$$

$$\begin{matrix} f(a_2, x_n^1 - X_2 + X_n) & \cdots & f(a_M, x_n^1 - X_M + X_n) \\ 0 & \cdots & f(a_M, x_n^2 - X_M + X_n) \\ \vdots & \cdots & \vdots \\ f(a_2, x_n^N - X_2 + X_n) & \cdots & 0 \end{matrix} \Bigg].$$

Therefore, by using Eqs. 33 and 49, the Chebyshev polynomial expansion coefficients of crack n, $\{c\}^n = \{c_1^n, c_2^n, \ldots, c_N^n\}^T$, can be determined by

$$[A]^n\{c\}^n = -\frac{1}{c_{44}^1\beta_0}(\{t\}_n^I + [Q]^n\{C\}). \tag{52}$$

$[A]^n$ is a known matrix given by (37) with the half-length of the crack a being replaced by a_n. Substituting (51) into (52), the governing equation for solving $\{C\}$ is obtained, from which $\{C\}$ can be determined.

The singular behaviour of interfacial crack n is characterized by the following stress intensity factors:

$$K_r^n = \lim_{x_n \to a_n} [\sqrt{2\pi(a_n - x_n)}\tau_{yz}(x_n)], \tag{53}$$

$$K_l^n = \lim_{x_n \to -a_n} [\sqrt{-2\pi(a_n + x_n)}\tau_{yz}(x_n)] \tag{54}$$

with r and l representing right and left tips of the crack. By using Eq. 38, the stress intensity factor at the right tip of crack n can be expressed in terms of c_j^n as being

$$K_{\mathrm{III}}^n = K_r^n = \sqrt{\pi a_n}\sum_{j=1}^{N} c_j^n. \tag{55}$$

5 Results and discussions

This section will be devoted to the determination of the effect of different parameters upon the dynamic stress intensity factor (SIF). It should be mentioned that the SIF induced by a time-harmonic load is in general a complex quantity. The stress intensity factor should be multiplied by $e^{-i\omega t}$ and then the real part should be taken to obtain the physically meaningful stress intensity factor. For convenience, only the amplitude of the obtained complex stress intensity factor, which is the same as the amplitude of the physical value, is considered in the following examples.

The incident wave considered is the so-called Love wave propagating in the x-direction. The antiplane displacement of this wave can be generally expressed as

$$w^I = \overline{w}(y)e^{-ik^s x}, \tag{56}$$

where $\overline{w}(y)$ is a known function and k^s is the wave number. By using boundary and continuity conditions, the resulting interfacial stress can be expressed as (Wang et al. 2001)

$$\tau^I_{yz}(x,0) = -\tau e^{-ik^s x}, \tag{57}$$

where $\tau = Ac_{44}\chi$ is the maximum shear stress with A being a constant and $\chi = \sqrt{(k^s)^2 - (k^1)^2}$. The shear stress given by (57) is used in Eq. 26 as the boundary condition at the crack surface in the determination of the stress field for subproblem (2).

5.1 The single crack solution

First, we restrict our attention to the single crack problem. Figure 2 shows the effect of the thickness of the layer upon the normalized stress intensity factor ($K^* = |K_{\mathrm{III}}/(\tau\sqrt{\pi a})|$). In this case, the material constants of the piezoelectric layer and the host medium are assumed to be (Wang et al. 2001):

the piezoelectric layer

$$c_{44} = 2.56 \times 10^{10}(\mathrm{Pa}), \qquad e_{15} = 10.5(\mathrm{C/m^2}),$$
$$\kappa_{11} = 7.0832 \times 10^{-9}(\mathrm{C/Vm}), \quad \rho = 7500(\mathrm{kg/m^3})$$

host medium

$$c^1_{44} = 8.39 \times 10^{10}(\mathrm{Pa}), \qquad \rho^1 = 7800(\mathrm{kg/m^3}).$$

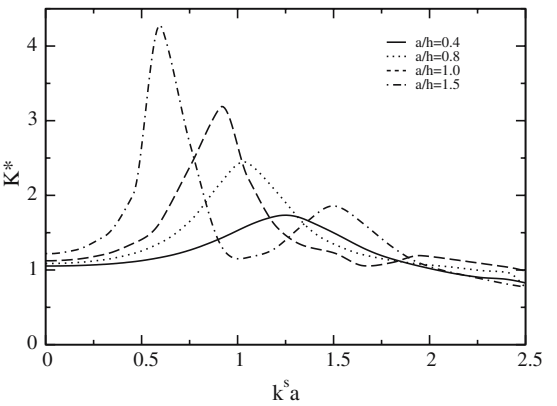

Fig. 2 The effect of the thickness of the layer upon the dynamic stress intensity factor of a single crack

When the frequency of the incident wave is low ($k^s a < 0.25$), the effect of the thickness of the layer upon K^* is insignificant for the cases considered. However, for higher frequencies the decrease of layer thickness will significantly intensify the dynamic overshoot phenomenon observed in traditional materials. This result indicates that relatively high-SIF may be generated for thin piezoelectric layers.

The piezoelectric effect can be expressed by using the following normalized piezoelectric constant $\lambda = e_{15}^2/\kappa_{11}c_{44}$. For the piezoelectric material currently used, $\lambda = 0.608$. Typically, for PZT-4 piezoceramics (Park and Sun 1994), λ can reach 0.977. In order to study the piezoelectric effect on the stress intensity factor, different λ values ranging from 0 to 1 are considered int he following example. Figure 3 shows the effect of λ on the normalized stress intensity factor for the case where $a/h = 1$, $\rho/\rho^1 = 1.0$. It can be seen clearly that λ significantly affects the frequencies at which maximum SIFs occur. The increase of the electromechanical coupling will result in the occurrence of maximum stress intensity factors at lower frequencies. When the loading frequency is high, this effect will reduce gradually.

The effect of material mismatch $q = c^1_{44}/c^*$ between the piezoelectric layer and the host medium on the dynamic stress intensity factor is shown in Fig. 4 for cases where $a/h = 1$ and $\rho/\rho^1 = 1.0$. The material properties of the piezoelectric layer is the same as that presented in Fig. 2 with $\lambda = 0.608$.

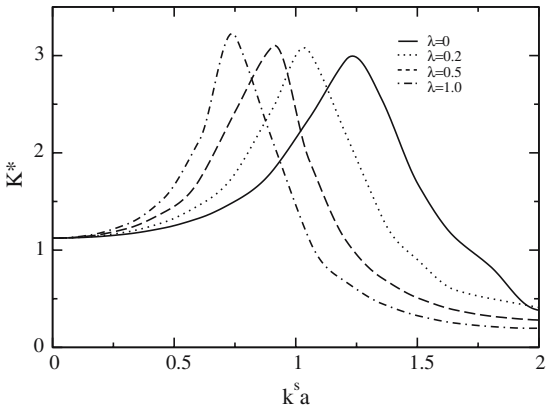

Fig. 3 The effect of the electromechanical coupling upon the dynamic stress intensity factor of a single crack

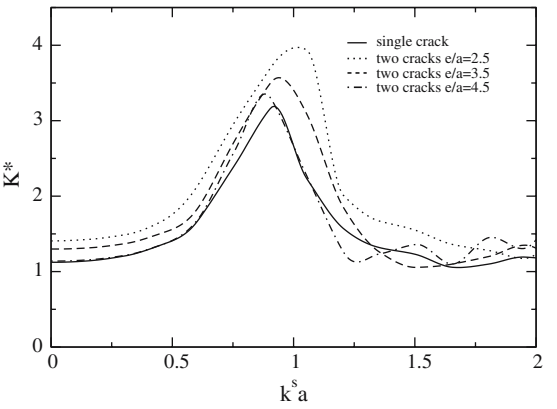

Fig. 5 The dynamic stress intensity factors of two interacting cracks

It is observed that q has a significant effect on the SIF for $0.5 < k^s a < 1.5$ although for low frequencies this effect is insignificant. With the increase of the material mismatch q the maximum normalized stress intensity factor occurs at a higher frequency and its amplitude increases.

5.2 The interacting cracks

Figure 5 shows the normalized dynamic stress intensity factor K^* at the inner tips of two identical cracks of length $2a$ with $a/h = 1$ subjected to the same incident wave discussed before. The material properties of the piezoelectric layer and the host medium are the same as those presented in Fig. 2. To evaluate the effect of crack interaction, different distances (e) between the centres of the two cracks are used with $e = 2.5a, e = 3.5a, e = 4.5a$, respectively. Significant interaction between these cracks is observed, even when the distance between cracks is similar to the crack length ($e/a = 3.5$). For closer cracks ($e/a = 2.5$), the stress intensity factor is increased dramatically in comparison with the corresponding single crack result.

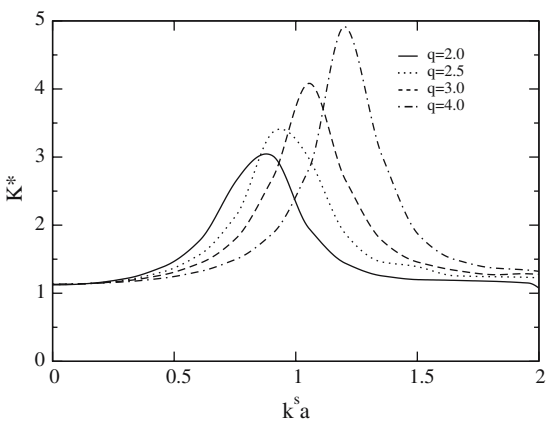

Fig. 4 The effect of the material mismatch upon the dynamic stress intensity factor of a single crack

Figure 6 shows the effect of the crack size upon the dynamic SIF K^* at the right tip of a crack with a half length $a = h$, which interacts to its right with a second crack with a half-length c. The material combination used is the same as the one in the previous example. The distance between the inner tips of the two cracks is assumed to be $d = 0.5a$. It can be observed that the SIF of the first crack increases with the increase of the size of the second crack, as well-known for traditional materials.

Figure 7 shows the effect of the electromechanical coupling (λ) on the normalized dynamic stress intensity factor K^* at the inner tips of two identical cracks of length $2a$ for the case where the material constants are the same as that used in Fig. 3 with $a/h = 1$. Similar to the single crack case shown in Fig. 3, With the increase of λ, the frequency at which the maximum amplitude of the SIF occurs decreases.

The normalized SIFs K^* at the right tips of three identical interacting cracks of length $2a$ are shown in Fig. 8, where the centres of the three cracks

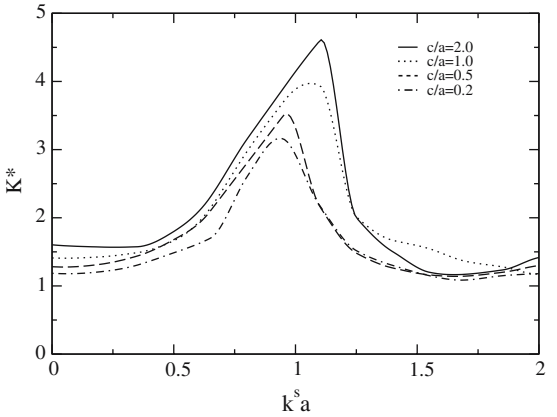

Fig. 6 The effect of the crack size upon the dynamic stress intensity factors of two interacting cracks

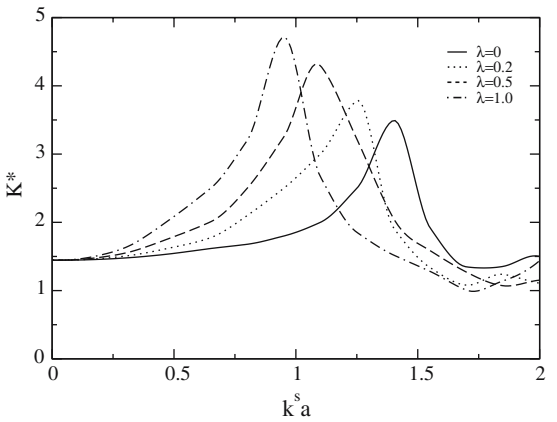

Fig. 7 The effect of the electromechanical coupling upon the dynamic stress intensity factors of two interacting cracks

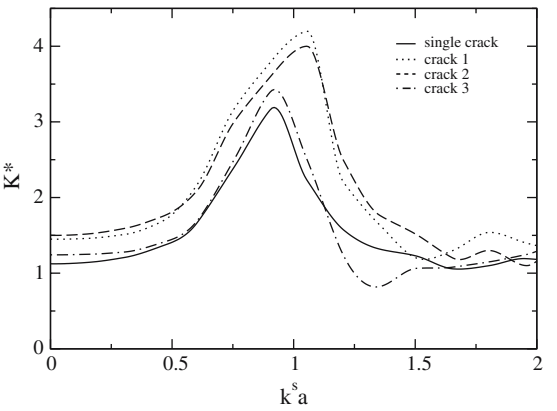

Fig. 8 The dynamic stress intensity factors of three interacting interfacial cracks

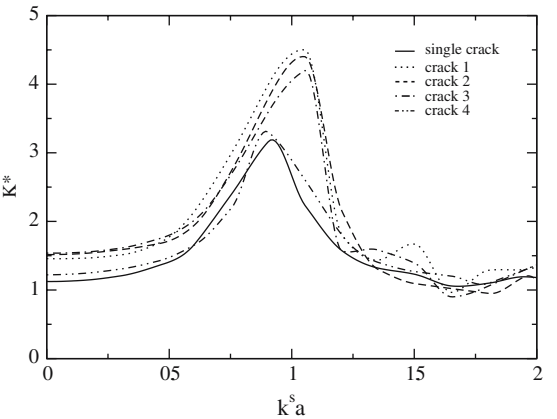

Fig. 9 The dynamic stress intensity factors of four interacting interfacial cracks

are located at $x = 0$, $x = 2.5a$, $x = 5.0a$, respectively. It is assumed that $a/h = 1$ and the material combination in the case presented in Fig. 2 is used. It is interesting to mention that the SIF at the outer tip of crack 3 is similar to that of a single crack, while the result of crack 1 is similar to that of crack 2. These results indicate that only the direct interaction between crack tips plays an important role even for the current dynamic problem. The stress intensity factor of crack 1 is close to that of crack 2 because only the inner tips are considered. This phenomenon can also be observed from the SIFs due to four identical interacting cracks of length $2a$, as shown in Fig. 9, where the centres of the four cracks are assumed to be at $x = 0$, $x = 2.5a$, $x = 5.0a$, $x = 7.5a$, respectively. Again the SIF of the outer tip (crack 4) is close to the single crack result and the stress intensity factors at all the inner tips (cracks 1–3) are quite similar. It can be concluded that the behaviour of this type of interfacial cracks is dominantly affected by the interaction between neighbouring cracks.

6 Concluding remarks

The dynamic behaviour of a piezoelectric layer bonded to an elastic medium containing multiple interfacial cracks subjected to steady state mechanical loads is investigated. The analysis is based on

the use of the integral transform method and a pseudo-incident wave method. Attention has been focussed on the study of the fundamental behaviour of the local stress field around crack tips. The effect of the geometry of the cracks, the material constants and the loading frequency of the incident Love wave upon the dynamic SIF is examined and discussed. The study reveals the important effect of the electromechanical coupling, material mismatch and geometry of the system upon the dynamic SIFs.

Acknowledgements The authors wish to acknowledge the Natural Sciences and Engineering Research Council of Canada (NSERC) for the financial support.

Appendix

The equation of motion and Gauss's law for a piezoelectric medium under antiplane loading are given by

$$\frac{\partial \tau_{xz}}{\partial x} + \frac{\partial \tau_{yz}}{\partial y} + \rho\omega^2 w = 0, \qquad \frac{\partial D_x}{\partial x} + \frac{\partial D_y}{\partial y} = 0,$$

where τ_{xz}, τ_{yz} are shear stress components, D_x and D_y are the electric displacements and w, ρ and ω are the antiplane displacement, mass density and frequency, respectively. Most existing piezoceramic materials are transversely isotropic, with the axis of symmetry being along the polarization direction. If the z-axis is chosen to be along this direction, the non-vanishing stress components (τ_{xz} and τ_{yz}) and the electric displacements (D_x and D_y) can be expressed as

$$\tau_{xz} = c_{44}\frac{\partial w}{\partial x} + e_{15}\frac{\partial \phi}{\partial x}, \qquad \tau_{yz} = c_{44}\frac{\partial w}{\partial y} + e_{15}\frac{\partial \phi}{\partial y}$$

and

$$D_x = e_{15}\frac{\partial w}{\partial x} - \kappa_{11}\frac{\partial \phi}{\partial x}, \qquad D_y = e_{15}\frac{\partial w}{\partial y} - \kappa_{11}\frac{\partial \phi}{\partial y},$$

where ϕ is the electric potential, c_{44}, e_{15} and κ_{11} are the elastic modulus, the piezoelectric constant and the dielectric constant of the medium, respectively. Substituting the constitutive equations into the equation of motion and Gauss's law results in

$$c_{44}\nabla^2 w + e_{15}\nabla^2\phi + \rho\omega^2 w = 0,$$
$$e_{15}\nabla^2 w - \kappa_{11}\nabla^2\phi = 0,$$

where the Laplacian operation ∇^2 stands for $\partial^2/\partial x^2 + \partial^2/\partial y^2$.

References

Bar-Cohen Y (2000) Emerging NDE technologies and challenges at the beginning of the 3rd millennium—Part I. Mater Eval 58(1):17–30

Beom H C (2003) Permeable cracks between two dissimilar piezoelectric materials. Int J Solids Struct 40:6669–6679

Boller C (2000) Next generation structural health monitoring and its integration into aircraft design. Int J Syst Sci 31:1333–1349

Chee C, Tong L, Steven GP (1998) A review on the modeling of piezoelectric sensors and actuators incorporated in intelligent structures. J Intell Mater Syst Struct 9:3–19

Chen YH, Han JJ (1999a) Macrocrack-microcrack interaction in piezoelectric materials, part I: basic formulations and J-analysis. J Appl Mech 66:514–521

Chen YH, Han JJ (1999b) Macrocrack-microcrack interaction in piezoelectric materials, part II: numerical results and discussions. J Appl Mech 66:522–527

Chen ZT, Karihaloo BL (1999) Dynamic response of a cracked piezoelectric ceramic under arbitrary electromechanical impact. Int J Solids Struct 36:5125–5133

Deeg WEF (1980) The analysis of dislocation, crack, and inclusion problems in piezoelectric solids. Ph.D thesis, Stanford University

Dunn M (1994) The effect of crack face boundary conditions on the fracture mechanics of piezoelectric solids. Eng Frac Mech 48:25–39

Gandhi MV, Thompson BS (1992) Smart materials and structures. Chapman Hall, London

Han XL, Wang ZC (1999) Interacting multiple cracks in piezoelectric materials. Int J Solids Struct 36:4183–4202

Li S, Mataga PA (1996a) Dynamic crack propagation in piezoelectric materials. Part 1: electrode solution. J Mech Phys Solids 44:1799–1830

Li S, Mataga PA (1996b) Dynamic crack propagation in piezoelectric materials. Part 1: vacuum solution. J Mech Phys Solids 44:1831–1866

Li XF, Fan TY, Wu XF (2000) A moving anti-plane crack at the interface between two dissimilar piezoelectric materials. Int J Eng Sci 38:1219–1234

Liu M, Hsia KJ (2003) Interfacial cracks between piezoelectric and elastic materials under in-plane electric loading. J Mech Phys Solids 51:921–944

Meguid SA, Wang XD (1998) Dynamic anti-plane behaviour of interacting cracks in a piezoelectric material. Int J Frac 91:391–403

Norita F, Shindo Y (1999) Scattering of antiplane shear waves by a finite crack in piezoelectric laminates. Acta Mech 134:27–43

Pak YE (1990) Crack extension force in a piezoelectric material. ASME J Appl Mech 57:615–627

Pak YE (1992) Linear electro-elastic fracture mechanics of piezoelectric materials. Int J Frac 54:79–100

Pak YE, Goloubeva E (1995) Influence of cracks on electroelastic properties of piezoelectric materials. Adaptive material systems AMD 206/MD 58, 33–43

Park S, Sun CT (1994) Crack extension in piezoelectric materials. SPIE 2189:357–368

Parton VZ (1976) Fracture mechanics of piezoelectric materials. Acta Astron 3:671–683

Shindo Y, Ozawa E (1990) Dynamic analysis of a cracked piezoelectric material. In: Hsieh RKT (ed) Mechanical modelling of new electromagnetic materials. Elsevier, Amsterdam, pp. 297–304

Suo Z, Kuo CM, Barnett DM, Willis JR (1992) Fracture mechanics for pieozoelectric ceramics. J Mech Phys Solids 40:739–765

Wang BL, Han JC, Du SY (2000) Electroelastic fracture dynamics for multi-layered piezoelectric materials under dynamic antiplane shearing. Int J Solids Struct 37:5219–5231

Wang Q, Quek ST, Varadan VK (2001) Love waves in piezoelectric coupled solid media. Smart Mater Struct 10:380–388

Wang XD (2001) On the dynamic behaviour of interacting interfacial cracks in piezoelectric media. Int J Solids Struct 38:815–831

Wang XD, Meguid SA (1997) Diffraction of SH-wave by interacting matrix crack and an inhomogeneity. ASME J Appl Mech 64:568–575

Wang XD, Meguid SA (2000) Modelling and analysis of the dynamic behaviour of piezoelectric materials containing interacting cracks. Mech Mater 32:723–737

Zhang TY, Qian CF, Tong P (1998) Linear electro-elastic analysis of a cavity or a crack in a piezoelectric material. Int J Solids Struct 35:2121–2149

Zhao XH, Meguid SA (2002) On the dynamic behaviour of a piezoelectric laminate with multiple interfacial collinear cracks. Int J Solids Struct 40:2477–2494